Research Article

A New Switching-Based Median Filtering Scheme and Algorithm for Removal of High-Density Salt and Pepper Noise in Images

V. Jayaraj and D. Ebenezer

*Digital Signal Processing Laboratory, Sri Krishna College of Engineering and Technology, Coimbatore,
Anna University Coimbatore, Tamilnadu 641008, India*

Correspondence should be addressed to V. Jayaraj, jayaraj_mevlsi@yahoo.co.in

A new switching-based median filtering scheme for restoration of images that are highly corrupted by salt and pepper noise is proposed. An algorithm based on the scheme is developed. The new scheme introduces the concept of substitution of noisy pixels by linear prediction prior to estimation. A novel simplified linear predictor is developed for this purpose. The objective of the scheme and algorithm is the removal of high-density salt and pepper noise in images. The new algorithm shows significantly better image quality with good PSNR, reduced MSE, good edge preservation, and reduced streaking. The good performance is achieved with reduced computational complexity. A comparison of the performance is made with several existing algorithms in terms of visual and quantitative results. The performance of the proposed scheme and algorithm is demonstrated.

1. Introduction

Images are often corrupted by impulsive noise in addition to several other types of noise. There are two models of impulsive noise, namely, salt, and pepper noise and random valued impulse noise. Salt and pepper noise is sometimes called fixed valued impulse noise producing two gray level values 0 and 255. Random valued impulse noise will produce impulses whose gray level value lies within a predetermined range. For example, if gray level exceeds a value L_{Max}, it is a positive impulse (L_{Max} to 255); if gray level is less than L_{Min}, it is a negative impulse (0 to L_{Min}). Impulse noise is caused by faulty camera sensors, faults in data acquisition systems, and transmission in a noisy channel. Median filtering has been established as a reliable method to remove impulse noise without damaging edge details [1, 2]. The Standard Median Filter (SMF) is effective only at low noise densities. Several methods have been proposed for removal of impulse noise at higher noise densities [3–5]. Recently, computational complexity has become an important consideration in impulse noise removal. Use of a small size fixed window in median filtering keeps the computational load a minimum. However, small window size leads to insufficient noise reduction.

Switching-based median filtering has been proposed as an effective alternative for reducing computational complexity. This method involves detection of noisy pixels prior to processing, and filtering is applied only to corrupted pixels while leaving uncorrupted pixels intact. Several switching-based methods have been proposed [6–21]. A recent method named Decision Based Algorithm (DBA) is one of the fastest methods and it is an efficient algorithm capable of impulse noise removal at noise densities as high as 80% [16, 17]. A major drawback of this algorithm is streaking at higher noise densities. The median filter not only smoothes the noise in homogeneous regions but it also tends to produce regions of constant or nearly constant intensity. The shape of these regions depends on the geometry of the filter window. They are usually streaks (linear patches) or amorphous blotches. These side effects of the median filter are highly undesirable, because they are perceived as either lines or contours that do not exist in the original image. The probability that two successive outputs of the median filter y_i, y_{i+1} have the same value is quite high

$$\Pr(y_i = y_{i+1}) = 0.5\left(1 - \left(\frac{1}{n}\right)\right) \tag{1}$$

when the input x_i is a stationary random process. When the window size "n" tends to infinity, this probability tends to 0.5. Streaking and blotching are undesirable effects. Postprocessing of the median filter output is desirable. A better solution is to use other nonlinear filters based on order statistics, which have better performance than median filter with reduced streaking and computational complexity. Streaking cannot be neglected particularly in high-density noise situations where a large number of pixels in a processing window are noisy pixels. One strategy, which is the simplest, is to replace the corrupted pixel by an immediate uncorrupted pixel. When window is moved to the next position, a similar situation arises. The replacement involves repetition of the uncorrupted pixel. This repetition causes streaking. In several algorithms such as adaptive algorithms and robust estimation algorithms, this repetition is less frequent and therefore is not as visible as in case of DBA. This paper introduces a new switching-based median filtering scheme and algorithm for removal of impulse noise with reduced streaking under the constraint of reduced computational complexity. The algorithm is also expected to provide good noise performance and edge preservation. This paper considers salt and pepper type impulse noise [12–17].

2. Switching-Based Median Filters

Switching-based median filters are well known. Identifying noisy pixels and processing only noisy pixels is the main principle in switching-based median filters. There are three stages in switching-based median filtering, namely, noise detection, estimation of noise-free pixels and replacement. The principle of identifying noisy pixels and processing only noisy pixels has been effective in reducing processing time as well as image degradation. The limitation of switching median filter is that defining a robust decision measure is difficult because the decision is usually based on a predefined threshold value. In addition the noisy pixels are replaced by some median value in their vicinity without taking into account local features such as presence of edges. Hence, edges and fine details are not recovered satisfactorily, especially when the noise level is high. In order to overcome these drawbacks. Chan et al. [16] have proposed a two-phase algorithm. In the first phase an adaptive median filter is used to classify corrupted and uncorrupted pixels. In the second phase, specialized regularization method is applied to the noisy pixels to preserve the edges besides noise suppression. The main drawback of this method is that the processing time is very high because it uses very large window size. There are several strategies for identification, processing, and replacement of noisy pixels. The simplest strategy is to replace the noisy pixels by the immediate neighborhood pixel. The DBA [17] employs this strategy wherein the computation time is the lowest among several standard algorithms even at higher noise densities. A disadvantage of this strategy is increased streaking. It is highly desirable to limit streaking which degrades the final processed image. This is indeed a challenging task under the constraint that the processing time be kept as low as possible while preserving edges and removing most of the noise.

3. New Switching-Based Median Filtering Scheme

This paper develops a new switching-based median filtering scheme for tackling the problem of streaking in switching-based median filters with minimal increase in computational load while preserving edges and removing most of the noise. The new scheme employs linear prediction in combination with median filtering. The proposed scheme is based on a new concept of substitution prior to estimation.

A linear predictive substitution of noisy pixels prior to estimation is proposed. The new scheme consists of four stages, namely, detection, substitution, estimation, and replacement in contrast to the existing schemes which work with three stages, namely, detection, estimation, and replacement.

Stage 1 takes pixels of the input image and identifies pixels corrupted by salt and pepper noise. Salt and pepper noise produces two-level pixels, namely, 0 and 255 and, therefore, identification is straightforward.

Stage 2 employs a simple modified first-order linear predictor whose output is used as a substitution for noisy pixels. It should be stated here that the linear predictor is not used as an estimator in strict sense. This new use of linear predictor is developed in the next section.

Stage 3 estimates denoised pixels. In order to preserve edges, a median filtering is employed that is based on L-estimators [1, 2]. The name L-estimators comes from linear combination of order statistics. An L-estimator can be defined as

$$Tn = \sum_{i=1}^{n} a_i x_i \qquad (2)$$

where x_i is the ith order statistic of the observation data. The performance of an L-estimator depends on its weights a_i which are some fixed coefficients.

Stage 4 replaces noisy pixels by the estimated pixels.

The methods chosen in each stage are strongly influenced by the goals, namely, good noise performance, reduced streaking, edge preservation, and minimal computational complexity.

4. Linear Predictive Substitution of Noisy Pixels

We consider the case where an image is corrupted by salt and pepper noise at high noise density levels such that more than half of the pixels inside a window (2D-representation) or inside an array (1D representation) are impulses of value 0 or 255. Noise-free pixels take on values between 0 and 255. For the purpose of analytical treatment, let X be a set $\{x_1, x_2, x_3, \ldots, x_j, x_{j+1}, x_{j+2}, \ldots, x_n\}$ consisting of original noise-free image pixels and x_{med} the median of X. Let Y be a set $\{y_1, y_2, y_3, \ldots, y_j, y_{j+1}, y_{j+2}, \ldots, y_n\}$ in which $y_1, y_2, y_3, \ldots, y_j$ are noise-free pixels, and $y_{j+1}, y_{j+2}, \ldots, y_n$ are pepper noise pixels. Let y_{med} be the median of Y. For simplicity, it is assumed that the elements of the set Y are arranged in ascending order of the values of

the pixels. Let Y be substituted by a new set $Z = \{y_1, y_2, y_3, \ldots, y_j, z_{j+1}, z_{j+2}, \ldots, z_n\}$ and z_{med} be the median of Z. The first j elements are noise-free pixels from set Y, and the rest of the elements from $z_{j+1}, z_{j+2}, \ldots, z_n$ are substitution pixels for the noisy pixels $y_{j+1}, y_{j+2}, \ldots, y_n$. These substitution pixels are derived from noise-free image pixels as developed in Section 5. In the case of high density noise levels above 50 percent, the median y_{med} is also a noisy pixel. Let $y_{j+1} \in Y$ by y_{med} and $z_{j+1} \in Z$ be replaced by z_{med}.

Proposition. *If more than half of the elements in the set Y are outliers, then*

$$\left\| x_{j+1} - z_{med} \right\| < \left\| x_{j+1} - y_{med} \right\|, \qquad (3)$$

where $\| \|$ represents the norm in L1 sense.

Proof. y_{j+1} is an impulse not correlated with y_j because the errors due to faulty operations do not depend on the original signal. Let $E[y_j \, y_{j+1}]$ be the autocorrelation $r_y(k)$. Let z_{j+1} be a substitute sample derived from one or more of the noise-free image pixels $y_1, y_2, y_3, \ldots, y_j$ such that z_{j+1} is a prediction. Let $E[y_j \, z_{j+1}]$ be the cross-correlation $r_z(k)$. Now, $r_z(k) > r_y(k)$. If $r_z(k) < r_y(k)$, then impulse noise sample y_{j+1} is correlated with y_j, and z_{j+1} is not correlated with y_j which is a contradiction. This is true for the subsequent elements in the sets Y and Z. Therefore, $\|x_{j+1} - z_{med}\| < \|x_{j+1} - y_{med}\|$. In other words, we propose that in the case of high density impulse noise levels, the median of a substitute set derived from noise-free pixels of the original set according to a predescribed rule that enhances correlation results in a denoised pixel $\qquad \square$

The next section develops a method for deriving substitute pixels for impulse noise pixels of a given corrupted image.

5. A Low-Order Recursive Linear Predictor from Finite Data

Linear prediction is the problem of finding the minimum mean square estimate of $x(n + 1)$ using a linear combination of the past p signal values from $x(n)$ to $x(n - p + 1)$. The most commonly used forward one step Finite Impulse Response (FIR) linear predictor of order $p - 1$ is given by

$$\hat{x}(n + 1) = \sum_{k=0}^{P-1} h(k)x(n - k) \qquad (4)$$

where $h(k)$ are the coefficients of the prediction filter. The solution is given by the Wiener-Hopf [18] equation

$$R_x(k)h(k) = r_x(k) \qquad (5)$$

where $R_x(k)$ is an autocorrelation matrix, $h(k)$ is predictor coefficient vector, and $r_x(k)$ is autocorrelation vector. The autocorrelation $R_x(k)$ is defined as

$$E[x(l - k)x(n - k)] = Rx(k - 1), \qquad \begin{matrix} k = 0 \text{ to } p - 1, \\ l = 0 \text{ to } p - 1, \end{matrix} \qquad (6)$$

$r_x(k)$ is defined as $r_x(k + 1) = E[x(n + 1)x(n - k)]$ for $k = 0$ to $p - 1$. It is assumed that signal values are real. Consider the set Y and let y_{j+1} be substituted by $\hat{y}_{j+1}$ which is a prediction from y_j or all previous elements. Let $\hat{y}_{j+1} = d_{j+1}$ so that d_{j+1} is the new substitute pixel for y_{j+1}. Now, let y_{j+2} be substituted by the prediction $\hat{d}_{j+1}$. Again, let $e_{j+2} = \hat{d}_{j+1}$. We substitute e_{j+2} for y_{j+3} and so on. The new set is now $Z = \{y_1, y_2, y_3, \ldots, y_j, d_{j+1}, e_{j+2}, \ldots, q_n\}$ wherein $d_{j+1}, e_{j+2}, \ldots, q_n$ are substitution pixels for noisy pixels by linear prediction from noise-free pixels. Rewriting $d_{j+1}, e_{j+2}, \ldots, q_n$ as $z_{i+1}, z_{i+2}, \cdot z_n$, we have $Z = \{y_1, y_2, y_3, \ldots, y_j, z_{i+1}, z_{i+2}, \ldots, z_n\}$. This is the substitution set introduced in Section 4.

The substitution concept proposed in this section requires a recursive-type prediction. One ideal approach is to start from a causal Infinite Impulse Response (IIR) linear predictor [18]. Suppose that the image can be modeled as an Auto Regressive Moving Average (ARMA) process with a known power spectrum $p(z)$ such that $p(z) = \sigma^2_0 Q(z)Q^*(1/z)$ where $Q(z)$ is the minimum phase spectral factor and σ^2_0 is the variance of the white noise driving the model. The causal Infinite Impulse Response (IIR) predictor is given by $H(z) = z(1 - 1/(Q(z)))$ which, in time domain, becomes

$$\hat{x}(n + 1) = \sum_{k=0}^{N-1} a_k \hat{x}(n - k) + \sum_{k=0}^{N-1} b_k x(n - k). \qquad (7)$$

In image processing with a short finite data, assumption of a power spectrum with known characteristics is generally not possible. The predictor coefficients can be determined from autocorrelation of the available data where signal model is not available. This is a reasonable approach in realistic situations [18].

Let $\hat{x}(n)$ be a prediction from one or more noise-free pixels. An outlier (a salt or pepper noise pixel) is substituted by $\hat{x}(n)$. This is acceptable because $\hat{x}(n)$ has some correlation with previous data and, therefore, is a better candidate than an impulse. After substitution, let $\hat{x}(n)$ be treated as an image pixel-free of impulse noise corruption. Let $\hat{x}(n)$ be $d(n)$. Define

$$E[\hat{x}(n)x(n + 1)] = E[d(n)x(n + 1)] = \hat{r}d(k). \qquad (8)$$

Let a first-order recursive linear predictor be defined as $\hat{x}(n + 1) = a_1 * \hat{x}(n) = a_1 * d(n)$. The error due to prediction is $e = x(n + 1) - \hat{x}(n + 1) = x(n + 1) - a_1 * d(n)$. Minimization of the square of the error leads to $\hat{r}d(k + 1) - a_1 * \hat{r}d(k) = 0$, $k = 0, 1, 2, \ldots$ where $a_1 = \hat{r}d(1)/\hat{r}d(0)$. The above procedure is repeated for all impulse corrupted pixels. All of the substitute pixels $Z_i, Z_{i+1}, \ldots, Zn$ are obtained by this procedure. The resulting set Z is a substitute set for X in this new scheme and not an estimate. We have proved in Section 4 that a subsequent optimization by median filtering of the substitute set takes the current noisy pixel closer to original noise-free image pixel. One of the computationally simplest optimizations that preserve edges is median filtering
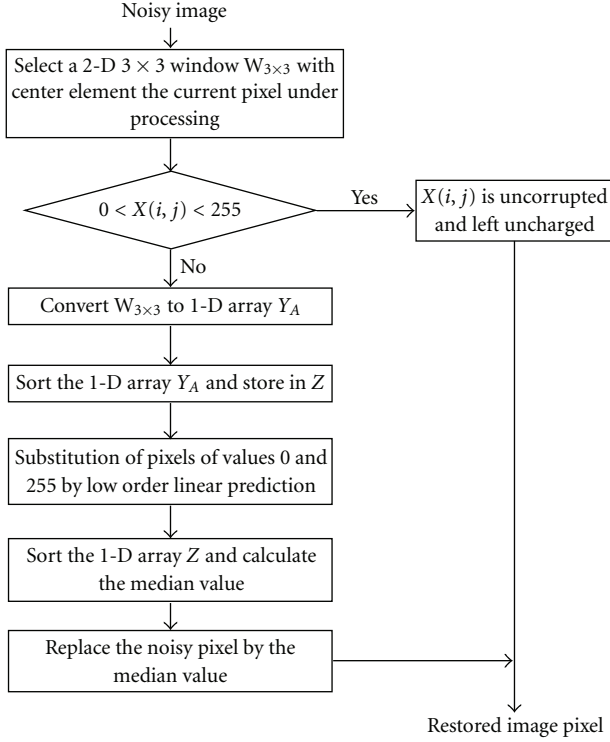
Noisy image

FIGURE 1: Flowchart of the proposed scheme.

and, therefore, the resulting substitute pixel set Z is filtered using median operation, which is an L1 optimization in Maximum Likelihood sense. Figure 1 shows the flow chart of the proposed scheme.

There are several advantages of the proposed scheme. In DBA the current noisy pixel under processing is replaced with the median of the processing window. If the median itself is corrupted, then the median is replaced by a previously processed neighborhood pixel. At higher noise densities most of the pixels will be corrupted necessitating repeated replacement. This repeated replacement produces streaking. The proposed method avoids this.

In robust statistics estimation filter [19–21], the current noisy pixel under processing is replaced by an image data estimated using an estimation algorithm. But the computation time is much longer. It will be demonstrated in Section 7 that the linear prediction substitution followed by median filtering as introduced by this paper can overcome the problem of streaking and blur while the computational complexity is reduced in comparison with robust statistics estimation filter.

6. The Proposed Noise Removal Algorithm

Let X denote the image corrupted by salt and pepper noise. For each pixel $X(i, j)$, a 2-D sliding window of size 3×3 is selected in such a way that the current pixel lies at the centre of the sliding window. The proposed algorithm first detects the noisy pixel. If the current processing pixel lies inside the dynamic range [0 255] then it is considered as a noise-free

pixel. Otherwise it is considered as a noisy pixel and replaced by a value using the proposed linear prediction algorithm.

Step 1. A 2-D window "$W_{3\times3}$" of size 3×3 is selected. Assume that current pixel under processing is $X(i, j)$.

Step 2. If $0 < X(i, j) < 255$, $X(i, j)$ is an uncorrupted pixel and it is left unchanged and the window slides to the next position.

Step 3. Else $X(i, j)$ is a corrupted pixel and go to Step 10.

Step 4. Store all the elements of "$W_{3\times3}$" in a 1-D array "Y_A".

Step 5. Sort the 1-D array "Y_A" in ascending order.

Step 6. For each pixel $x(n)$ in "Y_A" of value "255" moving from left to right, replace $x(n)$ by a predicted value which is given by $x(n) = \alpha \cdot x(n-1)$, where $\alpha = [R_{xx}(1)/R_{xx}(0)]$, $0 < \alpha < 1$ $R_{xx}(1)$, and $R_{xx}(0)$ are autocorrelation for lags 1 and 0.

Assuming stochastic approximation for maintaining simplest computational complexity

$$R_{xx}(1) = x(n-1) \cdot x(n-2), \qquad R_{xx}(0) = [x(n-1)]^2. \tag{9}$$

If $\alpha = 0$, substitute $x(n)$ by $x(n-1)$. (This is a special case when the pixel $x(n-2)$ is a salt noise pixel having the value 0.)

Step 7. For each pixel $x(n)$ in "Y_A" of value "0" moving from right to left, replace $x(n)$ by a predicted value which is given by, $x(n) = \alpha \cdot x(n+1)$, where $\alpha = [(R_{xx}(1))/(R_{xx}(0))]$, $0 < \alpha < 1$,

$$R_{xx}(1) = x(n+1) \cdot x(n+2), \qquad R_{xx}(0) = [x(n+1)]^2 \tag{10}$$

If $\alpha \geq 1$, substitute $x(n)$ by $x(n+1)$. (This is a special case when the pixel $x(n+2)$ is a pepper noise pixel having the value 255.)

Step 8. The new array is Z_A. Sort the 1-D array "Z_A" with predicted values and find the median value.

Step 9. Replace the current pixel $X(i, j)$ under processing by the above median value.

Step 10. Steps 1 to 3 are repeated until processing is completed for the entire image.

7. Illustration of the Proposed Algorithm

Each and every pixel of the image is checked for the presence of salt and pepper noise pixel. During processing if a pixel element lies between "0 and 255", it is left unchanged. If the value is 0 or 255, then it is a noisy pixel and it is substituted by a substitution pixel.

Array labeled Y_1 displays an image corrupted by salt and pepper noise.

Array labeled Y_2 depicts the current processing window and a pepper noise pixel. The square shown in solid line represents the window; and element inside the circle represents a pepper noise pixel

$$Y_1 = \begin{array}{|c|c|c|c|c|} \hline 20 & 189 & 178 & 160 & 199 \\ \hline 210 & 200 & 205 & 188 & 234 \\ \hline 168 & 169 & 255 & 255 & 0 \\ \hline 0 & 255 & 255 & 255 & 0 \\ \hline 0 & 0 & 255 & 0 & 255 \\ \hline \end{array}$$

$$Y_2 = \begin{array}{|c|c|c|c|c|} \hline 200 & 189 & 178 & 160 & 199 \\ \hline 210 & 200 & 205 & 188 & 234 \\ \hline 168 & 199 & 255 & 255 & 0 \\ \hline 0 & 255 & 255 & 255 & 0 \\ \hline 0 & 0 & 255 & 0 & 255 \\ \hline \end{array}$$

If the current pixel under processing is between 0 and 255, it is left unchanged. Otherwise it will be replaced by a new pixel value estimated using the proposed algorithm. For this purpose, the elements inside processing window are arranged as an array Y_A and sorted in ascending order

$$Y_A = \begin{array}{|c|c|c|c|c|c|c|c|c|} \hline 169 & 188 & 200 & 205 & 255 & 255 & 255 & 255 & 255 \\ \hline \end{array}$$

$$Z_A = \begin{array}{|c|c|c|c|c|c|c|c|c|} \hline 169 & 188 & 200 & 205 & 200 & 255 & 255 & 255 & 255 \\ \hline \end{array}$$

Check for the pixel elements of value "255" starting from the left. If the pixel value is "255", then that value will be substituted by a predicted value from the immediate neighborhood pixel. Array Z_A illustrates this. The element inside the circle is the substitute pixel for the pepper noise pixel. This is repeated for all the pixels having the value "255". Array Z_A is sorted again to find the median. This is shown as array Z_D. The element encircled is the median

$$Z_D = \begin{array}{|c|c|c|c|c|c|c|c|c|} \hline 169 & 188 & 200 & 200 & 200 & 200 & 205 & 205 & 205 \\ \hline \end{array}$$

$$Z_P = \begin{array}{|c|c|c|c|c|} \hline 200 & 189 & 178 & 160 & 199 \\ \hline 210 & 200 & 205 & 188 & 234 \\ \hline 168 & 199 & 200 & 255 & 0 \\ \hline 0 & 255 & 255 & 255 & 0 \\ \hline 0 & 0 & 255 & 0 & 255 \\ \hline \end{array}$$

Finally, the current noisy pixel in the window in array Y_2 is replaced with the new median value. The final processed array is shown as Z_P.

The element encircled in array Z_P is the final estimate of the pepper noise pixel of array Y_2. In the proposed algorithm, a 3×3 window will slide over the entire image. Computation complexity is minimum with a 3×3 fixed window. This procedure is repeated for the entire image. Similar procedure can be adopted for the salt noise substitution, estimation, and replacement.

8. Simulation Results and Discussion

In this section, results are presented to illustrate the performance of the proposed algorithm. Images are corrupted by uniformly distributed salt and pepper noise at different densities for evaluating the performance of the algorithm. Three images are selected. They are Lena, Cameraman, and Boat image. A quantitative comparison is performed between several filters and the proposed algorithm in terms of Peak Signal-to-Noise Ratio (PSNR), Mean Square Error (MSE), Image Enhancement Factor (IEF), Mean Structural SIMilarity (MSSIM) Index, and computational time. The results show improved performance of the proposed algorithm in terms of these measures. Matlab R2007b on a PC equipped with 2.21 GHz CPU and 2 GB RAM has been used for evaluation of computation time of all algorithms.

The performance of the algorithm for various images at different noise levels from 70% to 90% is studied, and results are shown in Figures 2–7. The metrics for comparison are defined as follows:

$$\text{PSNR} = 10 \log 10 \left(\frac{255^2}{\text{MSE}} \right),$$

$$\text{MSE} = \frac{1}{MN} \sum_{i=1}^{M} \sum_{j=1}^{N} (rij - xij)^2,$$

$$\text{IEF} = \frac{\sum_{i=1}^{M} \sum_{j=1}^{N} \left(n_{ij} - r_{ij} \right)^2}{\sum_{i=1}^{M} \sum_{j=1}^{N} \left(x_{ij} - r_{ij} \right)^2}, \quad (11)$$

$$\text{SSIM}(r,x) = \frac{(2\mu_r\mu_x + C_1)(2\sigma_{xy} + C_2)}{(\mu_r^2 + \mu_x^2 + C_1)(\sigma_r^2 + \sigma_x^2 + C_2)},$$

$$\text{MSSIM}(R,X) = \frac{1}{G} \sum_{p=1}^{G} \text{SSIM}\left(r_p, x_p \right).$$

where r_{ij} is the original image, x_{ij} is the restored image, and n_{ij} is the corrupted image. The Structural SIMilarity index between the original image and restored image is given by SSIM [21] where μ_r and μ_x are mean intensities of original and restored images, σ_r and σ_x are standard deviations of original and restored images, r_p and x_p are the image contents of pth local window, and G is the number of local windows in the image. Figure 2 displays the original and corrupted images of Lena.jpg image. Figure 4 displays the original and corrupted images of Boat.gif image. Figure 6 displays the original and corrupted images of Cameraman.tif image.

In Figures 3, 5 and 7, the first column represents the output of Standard Median Filter (SMF) [4], second column represents the output of Progressive Switching Median Filter (PSMF) [14], third column represents the output of Adaptive Median Filter (AMF) [16], and fourth column represents the output of Decision-Based Algorithm (DBA) [17]. Fifth column represents the output of Robust Estimation Median Filter (REMF) [19] and the sixth column represents the output of the Proposed Algorithm (PA). Tables 1–6 display the quantitative measures. SMF replaces the current pixel

TABLE 1: PSNR and MSE for various filters for Lena image at different noise densities.

Noise density (%)	PSNR						MSE					
	SMF	PSMF	AMF	DBA	REMF	PA	SMF	PSMF	AMF	DBA	REMF	PA
20	29.039	32.379	37.561	37.476	38.204	40.188	81.126	37.6033	11.4017	11.6275	9.8338	9.1702
50	15.095	20.997	30.061	30.249	31.499	32.942	2011..9	516.869	64.1182	61.4046	46.050	41.5837
70	9.861	9.884	25.509	25.737	27.228	28.133	6713.6	6679.1	182.901	173.518	123.09	99.9569
80	7.926	7.983	22.975	22.936	24.702	25.836	10482	10346	327.752	330.747	220.25	169.607
90	6.441	6.485	19.283	19.770	21.355	24.316	14739	14609	767.042	685.698	476.01	240.925

TABLE 2: IEF and MSSIM for various filters for Lena image at different noise densities.

Noise density (%)	IEF						MSSIM					
	SMF	PSMF	AMF	DBA	REMF	PA	SMF	PSMF	AMF	DBA	REMF	PA
20	47.757	102.53	338.13	331.43	391.56	398.51	0.081	0.932	0.975	0.974	0.978	0.990
50	4.811	18.692	150.17	157.32	209.35	241.55	0.025	0.570	0.899	0.898	0.924	0.940
70	2.014	2.024	74.156	78.265	110.14	155.65	0.012	0.054	0.790	0.796	0.852	0.883
80	1.481	1.494	47.199	46.653	70.085	100.74	0.009	0.026	0.708	0.708	0.790	0.860
90	1.183	1.188	22.669	25.360	36.483	88.383	0.005	0.011	0.568	0.583	0.683	0.812

TABLE 3: PSNR and MSE for various filters for Boat image at different noise densities.

Noise density (%)	PSNR						MSE					
	SMF	PSMF	AMF	DBA	REMF	PA	SMF	PSMF	AMF	DBA	REMF	PA
20	27.091	30.110	34.840	34.706	35.256	38.428	127.06	63.396	21.334	22.004	19.387	16.632
50	15.074	20.406	27.820	27.842	28.985	31.393	2021.5	592.166	107.408	106.867	82.137	64.782
70	9.889	9.833	23.726	23.730	24.143	26.775	6671.3	6557.700	275.748	275.461	198.95	152.041
80	7.966	7.959	21.198	21.552	22.865	24.555	10388	10404.00	493.466	454.861	336.19	266.823
90	6.542	6.558	17.942	18.294	19.369	22.220	14416	14363.000	1044.500	963.108	751.93	389.985

TABLE 4: IEF and MSSIM for various filters for boat image at different noise densities.

Noise density (%)	IEF						MSSIM					
	SMF	PSMF	AMF	DBA	REMF	PA	SMF	PSMF	AMF	DBA	REMF	PA
20	30.185	59.774	176.77	172.65	196.61	204.95	0.109	0.918	0.970	0.970	0.973	0.982
50	4.685	15.975	88.062	88.574	115.02	126.85	0.035	0.576	0.879	0.878	0.903	0.951
70	1.989	1.974	47.993	48.274	66.722	77.234	0.017	0.065	0.754	0.756	0.807	0.912
80	1.466	1.464	30.766	33.230	45.331	53.011	0.011	0.032	0.657	0.665	0.726	0.839
90	1.184	1.186	16.361	17.689	22.783	41.416	0.007	0.016	0.518	0.531	0.600	0.787

TABLE 5: PSNR and MSE for various filters for Cameraman image at different noise densities.

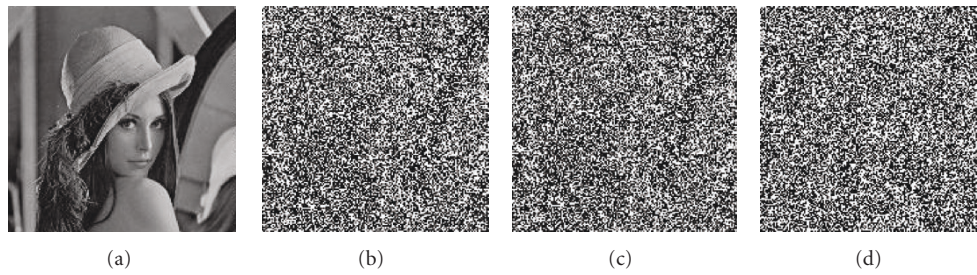| Noise density (%)	PSNR						MSE					
	SMF	PSMF	AMF	DBA	REMF	PA	SMF	PSMF	AMF	DBA	REMF	PA
20	23.987	25.101	30.973	30.401	31.058	34.009	259.64	200.880	51.976	59.292	50.972	28.544
50	14.417	18.507	24.212	24.034	24.671	25.933	2351.5	917.025	246.554	256.824	221.80	147.737
70	9.455	9.397	20.944	20.580	21.893	23.686	7372.7	7471.200	523.252	568.926	420.55	297.153
80	7.768	7.719	18.328	18.621	19.659	22.700	10871.	10996.000	18.328	893.218	703.41	357.309
90	6.169	6.202	15.621	16.591	17.103	22.151	15711.	15592.000	1782.500	1425.600	1267.0	436.059

(a) (b) (c) (d)

FIGURE 2: (a) Original Lena image. (b) Image corrupted by 70% noise density. (c) Image corrupted by 80% noise density. (d) Image corrupted by 90% noise density.
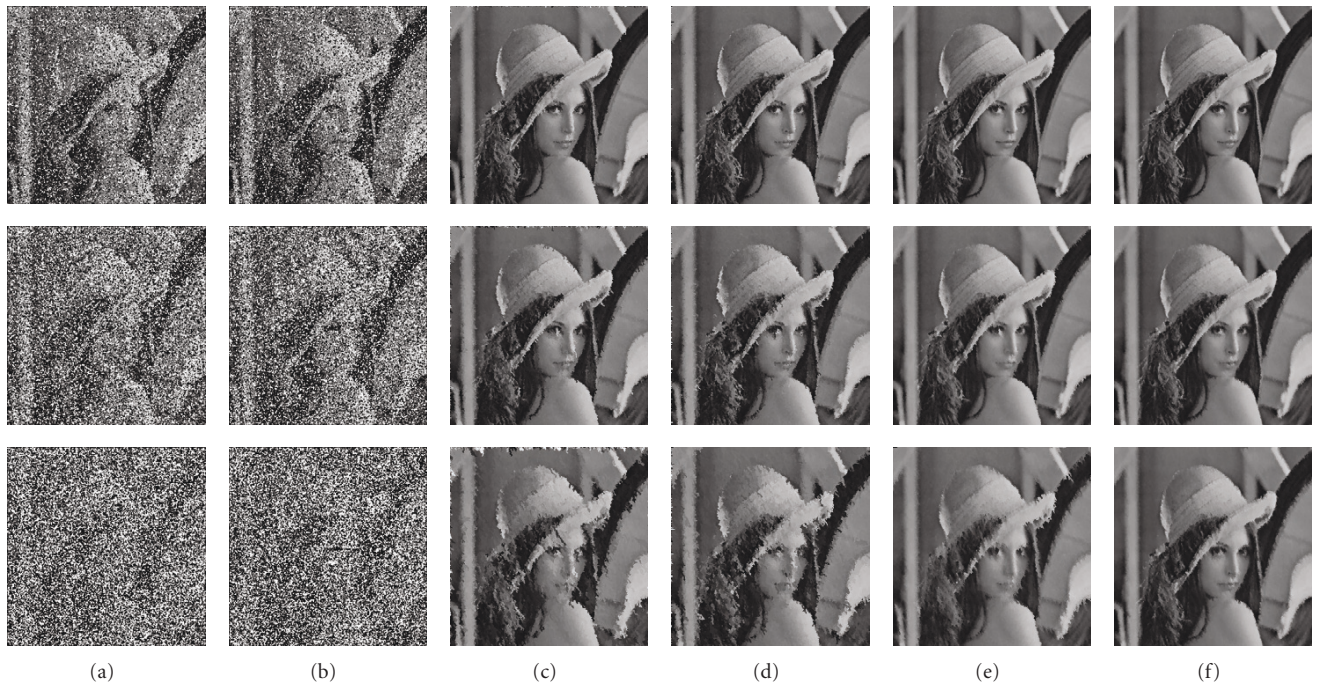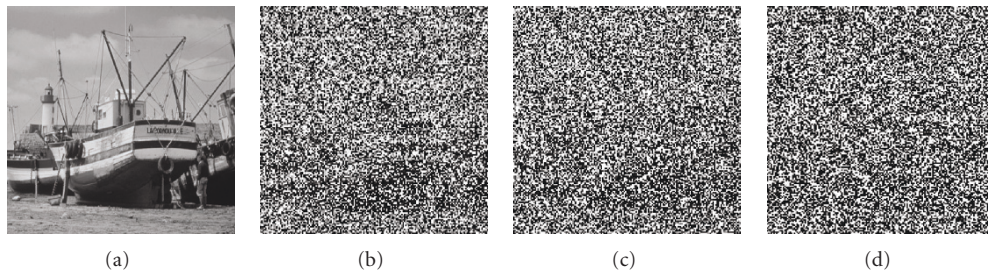

(a) (b) (c) (d) (e) (f)

FIGURE 3: Results of different filters for Lena image. (a) Output of SMF. (b) Output of PSMF. (c) Output of AMF. (d) Output of DBA. (e) Output of REMF. (f) Output of PA. Row 1–Row 3 show processed results of various filters for Lena.jpg image corrupted by 70%, 80%, and 90% noise densities.

(a) (b) (c) (d)

FIGURE 4: (a) Original Boat image. (b) Image corrupted by 70% noise density. (c) Image corrupted by 80% noise density. (d) Image corrupted by 90% noise density.

TABLE 6: IEF and MSSIM for various filters for cameraman image at different noise densities.

Noise density (%)	IEF						MSSIM					
	SMF	PSMF	AMF	DBA	REMF	PA	SMF	PSMF	AMF	DBA	REMF	PA
20	15.451	19.597	79.626	67.752	73.015	98.192	0.137	0.902	0.966	0.963	0.966	0.986
50	4.293	11.092	41.427	39.008	45.476	66.712	0.048	0.569	0.871	0.868	0.883	0.949
70	1.920	1.902	27.092	25.021	33.443	45.143	0.026	0.071	0.758	0.757	0.795	0.884
80	1.484	1.461	16.948	18.203	22.947	39.644	0.017	0.040	0.668	0.675	0.718	0.860
90	1.165	1.167	10.223	12.729	14.327	36.718	0.008	0.018	0.541	0.586	0.619	0.848

TABLE 7: Comparison of PSNR and CPU time in seconds for cameraman image.

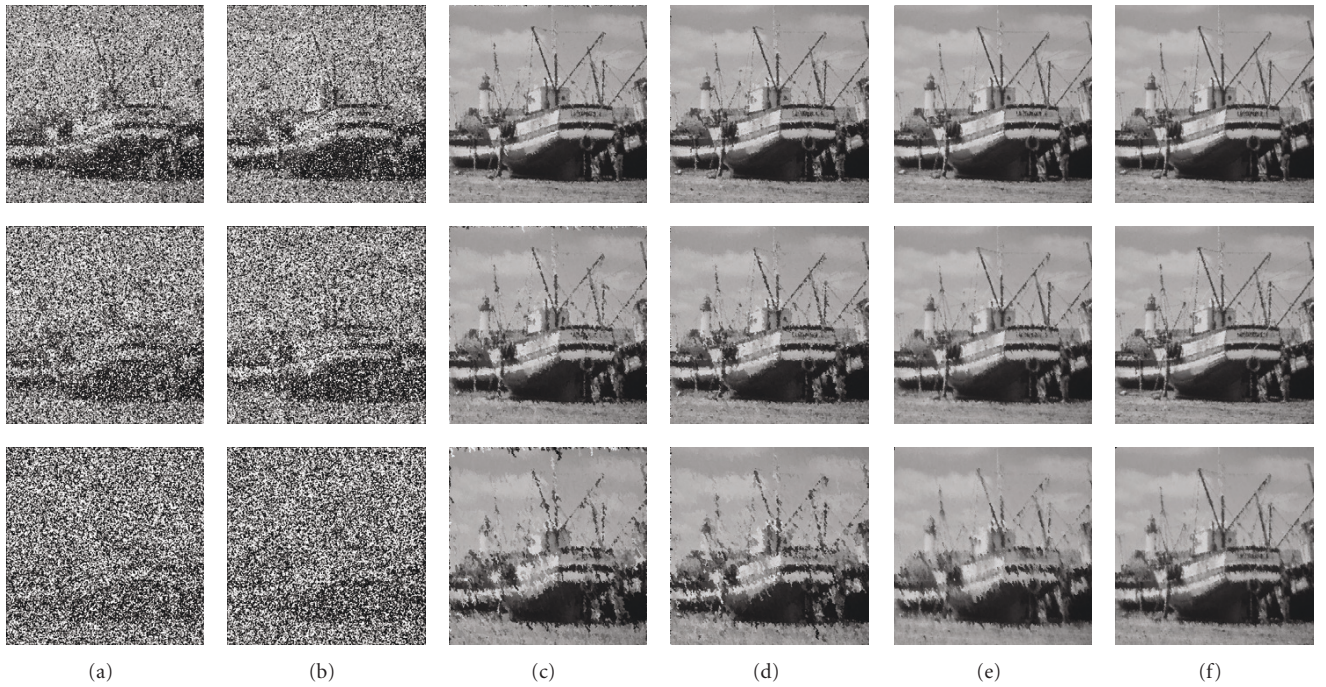| Method	Noise density = 70%		Noise density = 80%		Noise density = 90%	
	PSNR	Time	PSNR	Time	PSNR	Time
SMF	9.8887	0.1043	7.9656	0.1055	6.5424	0.1111
Raymond H.Chan et al.	23.7257	38.4543	21.1982	44.4529	17.9415	51.0610
DBA	23.7302	5.6979	21.552	5.6357	18.2941	5.7585
REMF	24.1434	17.9368	22.8649	20.4194	19.369	23.0306
PA	26.7745	6.8083	24.5547	7.7198	22.2203	8.8524

FIGURE 5: Results of different filters for Boat image. (a) Output of SMF. (b) Output of PSMF. (c) Output of AMF. (d) Output of DBA. (e) Output of REMF. (f) Output of PA. Row 1–Row 3 show processed results of various filters for Boat.gif image corrupted by 70%, 80%, and 90% noise densities.

by its median value irrespective of whether a pixel is corrupted or not. Therefore, the performance is poor. PSMF has slightly improved performance but its noise removing capacity is very poor at higher noise densities. AMF exhibits improved performance but due to its adaptive nature the computation complexity is much higher. DBA has very good noise removing capability and good edge preservation at higher noise densities but it produces streaking at higher noise densities. REMF has improved performance than DBA but its computational complexity is much higher. Figures
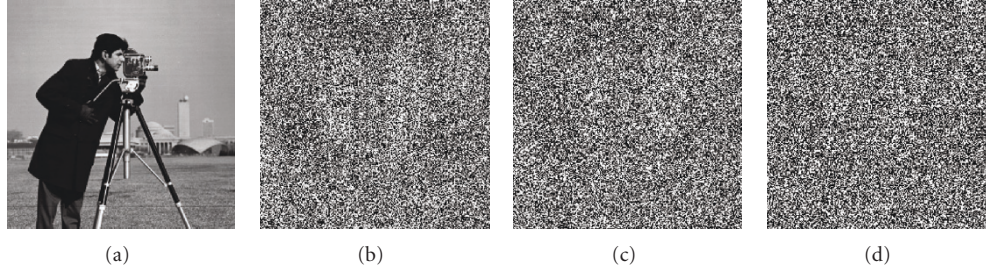
FIGURE 6: (a) Original Cameraman image. (b) Image corrupted by 70% noise density. (c) Image corrupted by 80% noise density. (d) Image corrupted by 90% noise density.
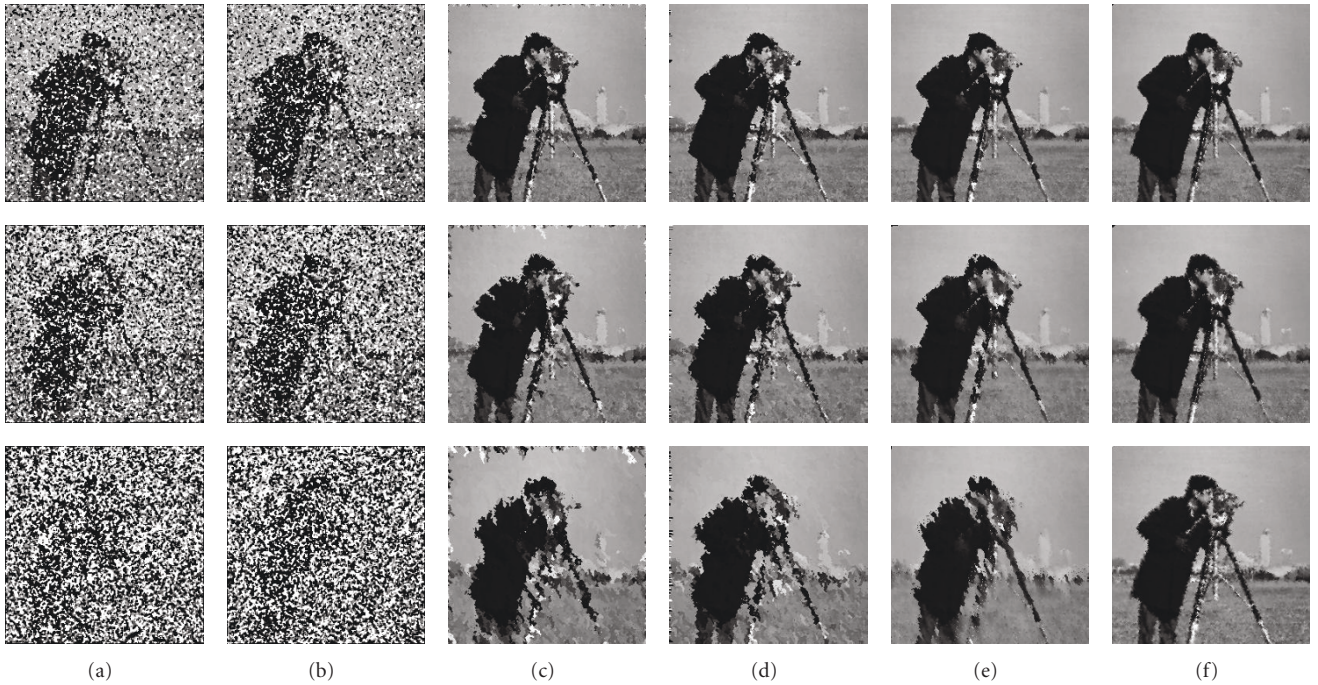

FIGURE 7: Results of different filters for Cameraman image. (a) Output of SMF. (b) Output of PSMF. (c) Output of AMF. (d) Output of DBA. (e) Output of REMF. (f) Output of PA. Row 1–Row 3 show processed results of various filters for Cameraman.tif image corrupted by 70%, 80%, and 90% noise densities.

8–11 display the quantitative performance of the various algorithms for cameraman image. It can be observed that the proposed algorithm removes noise effectively even at higher noise levels and preserves the edges and reduces streaking which is a major drawback of DBA while maintaining lower computational complexity when compared to adaptive algorithm and robust statistics-based algorithms. Figure 12 represents the computation time required at various noise densities for different algorithms on cameraman image, and the results are also tabulated in Table 7.

In the proposed method, replacement by immediate neighborhood is avoided by substitution of noisy pixels potential candidates based on linear prediction. Since linear prediction is employed prior to any processing, repetition of the same pixel is avoided as window is moved from one position to the next position. This eliminates streaking. In the standard switching median filtering except DBA, estimation of noise-free pixels takes considerable time on account of mathematical criteria employed. This time increases significantly in adaptive based estimation techniques. In the proposed filter, the estimation is not based on explicit computation of estimation criteria; instead a median filtering replaces estimation. This is the main reason for reduction in computational complexity. Extra computation necessitated by low-order linear prediction is significantly smaller than techniques employing rigorous estimation schemes. The DBA which is one of the fastest algorithms (which also avoids estimation) involves three median sorting, namely, right sorting, left, and diagonal sorting. In the proposed filter there is only two sortings. Therefore introduction
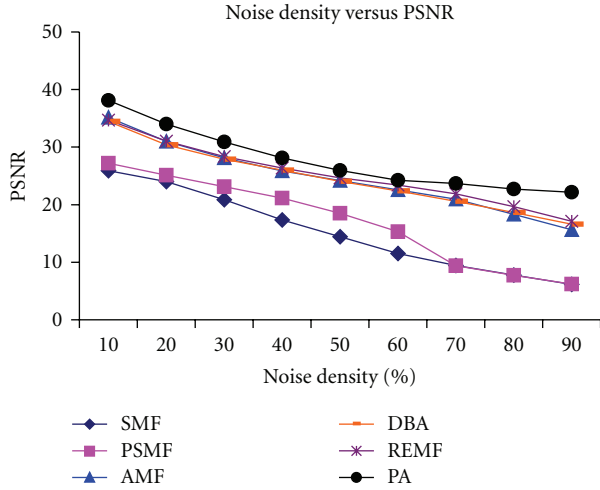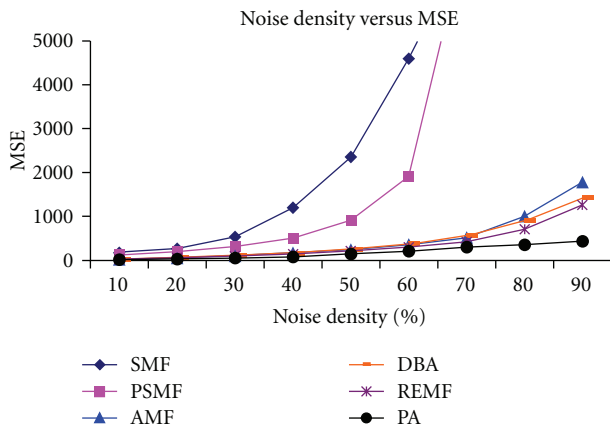
Noise density versus PSNR

FIGURE 8: Noise density versus PSNR for cameraman image.

Noise density versus MSE

FIGURE 9: Noise density versus MSE for cameraman image.

Noise density versus IEF
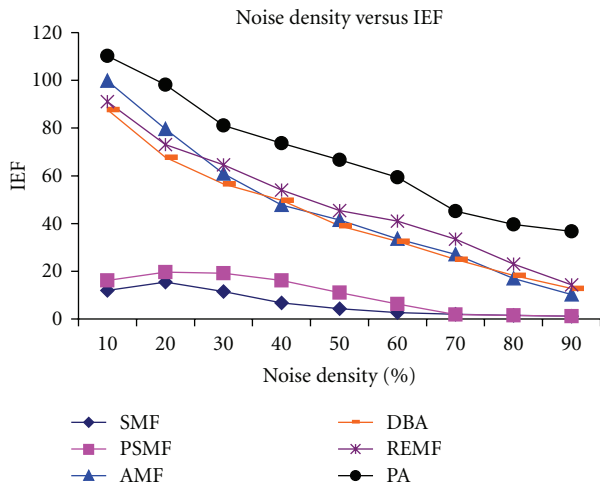

FIGURE 10: Noise density versus IEF for cameraman image.

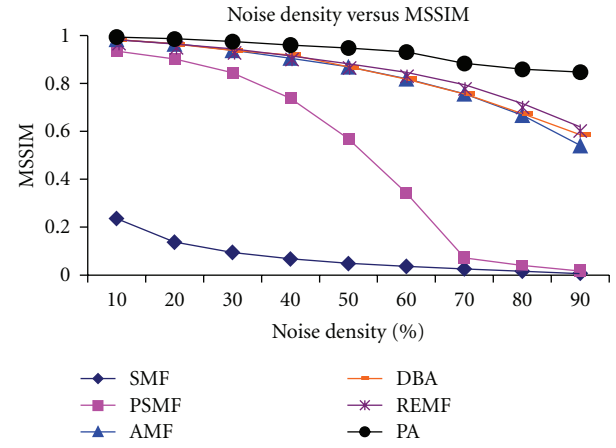Noise density versus MSSIM

FIGURE 11: Noise density versus MSSIM for Cameraman image.
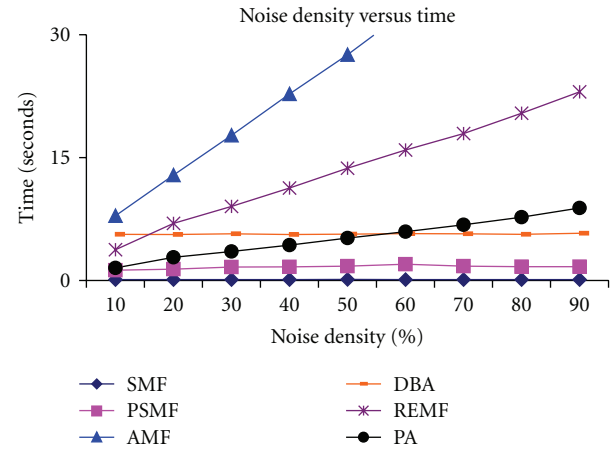
Noise density versus time

FIGURE 12: Noise density versus computation time in seconds for Cameraman image.

of first-order linear prediction only slightly increases the computation time compared with DBA but much lower than other filters. The proposed algorithm can be a good compromise in preference to the adaptive algorithm, DBA, and robust statistics-based algorithm.

9. Conclusion

A new switching-based median filtering scheme and an algorithm for removal of high-density salt and pepper noise in images is proposed. The algorithm is based on a new concept of substitution prior to estimation in contrast to the standard switching-based nonlinear filters. Noisy pixels are substituted by prediction prior to estimation. A simple novel recursive linear predictor is developed for this purpose. A subsequent optimization by median filtering results in final estimates. The performance of the algorithm is compared with that of SMF, PSMF, AMF, DBA, and REMF in terms of Peak Signal-to-Noise Ratio, Mean Square Error, Mean Structure Similarity Index, and Image Enhancement Factor and Computational time. Both visual and quantitative results

are demonstrated. The results show that the notable features of the proposed algorithm are reduced streaking at high noise densities compared to DBA which is one of the fastest algorithm and reduced computational complexity compared to adaptive and robust algorithms. The proposed algorithm can be a good compromise for salt and pepper noise removal in images at high noise densities. However, further reduction in computational complexity is desirable.

References

[1] I. Pitas and A. N. Venetsanopoulos, *Nonlinear Digital Filters Principles and Applications*, Kluwer Academic Publishers, Norwell, Mass, USA, 1990.

[2] J. Astola and P. Kuosmanen, *Fundamentals of Nonlinear Digital Filtering*, CRC Press, Boca Raton, Fla, USA, 1997.

[3] N. C. Gallagher Jr. and G. L. Wise, "A theoretical analysis of the properties of median filters," *IEEE Transactions on Acoustics, Speech, and Signal Processing*, vol. 29, no. 6, pp. 1136–1141, 1981.

[4] T. A. Nodes and N. C. Gallagher Jr., "Median filters: some modifications and their properties," *IEEE Transactions on Acoustics, Speech, and Signal Processing*, vol. 30, no. 5, pp. 739–746, 1982.

[5] E. Abreu, M. Lightstone, S. K. Mitra, and K. Arakawa, "A new efficient approach for the removal of impulse noise from highly corrupted images," *IEEE Transactions on Image Processing*, vol. 5, no. 6, pp. 1012–1025, 1996.

[6] D. R. K. Brownrigg, "The weighted median filter," *Communications of the ACM*, vol. 27, no. 8, pp. 807–818, 1984.

[7] O. Yli-Harja, J. Astola, and Y. Neuvo, "Analysis of the properties of median and weighted median filters using threshold logic and stack filter representation," *IEEE Transactions on Signal Processing*, vol. 39, no. 2, pp. 395–410, 1991.

[8] G. R. Arce and J. L. Paredes, "Recursive weighted median filters admitting negative weights and their optimization," *IEEE Transactions on Signal Processing*, vol. 48, no. 3, pp. 768–779, 2000.

[9] Y. Dong and S. Xu, "A new directional weighted median filter for removal of random-valued impulse noise," *IEEE Signal Processing Letters*, vol. 14, no. 3, pp. 193–196, 2007.

[10] T. Chen, K.-K. Ma, and L.-H. Chen, "Tri-state median filter for image denoising," *IEEE Transactions on Image Processing*, vol. 8, no. 12, pp. 1834–1838, 1999.

[11] H. Hwang and R. A. Haddad, "Adaptive median filters: new algorithms and results," *IEEE Transactions on Image Processing*, vol. 4, no. 4, pp. 499–502, 1995.

[12] S. Zhang and M. A. Karim, "A new impulse detector for switching median filters," *IEEE Signal Processing Letters*, vol. 9, no. 11, pp. 360–363, 2002.

[13] H.-L. Eng and K.-K. Ma, "Noise adaptive soft-switching median filter," *IEEE Transactions on Image Processing*, vol. 10, no. 2, pp. 242–251, 2001.

[14] Z. Wang and D. Zhang, "Progressive switching median filter for the removal of impulse noise from highly corrupted images," *IEEE Transactions on Circuits and Systems II*, vol. 46, no. 1, pp. 78–80, 1999.

[15] P.-E. Ng and K.-K. Ma, "A switching median filter with boundary discriminative noise detection for extremely corrupted images," *IEEE Transactions on Image Processing*, vol. 15, no. 6, pp. 1506–1516, 2006.

[16] R. H. Chan, C.-W. Ho, and M. Nikolova, "Salt-and-pepper noise removal by median-type noise detectors and detail-preserving regularization," *IEEE Transactions on Image Processing*, vol. 14, no. 10, pp. 1479–1485, 2005.

[17] K. S. Srinivasan and D. Ebenezer, "A new fast and efficient decision-based algorithm for removal of high-density impulse noises," *IEEE Signal Processing Letters*, vol. 14, no. 3, pp. 189–192, 2007.

[18] M. H. Hayes, *Statistical Digital Signal Processing and Modeling*, John Wiley & Sons, Singapore, 2002.

[19] S. Schulte, M. Nachtegael, V. DeWitte, D. van der Weken, and E. E. Kerre, "A fuzzy impulse noise detection and reduction method," *IEEE Transactions on Image Processing*, vol. 15, no. 5, pp. 1153–1162, 2006.

[20] A. Ben Hamza and H. Krim, "Image denoising: a nonlinear robust statistical approach," *IEEE Transactions on Signal Processing*, vol. 49, no. 12, pp. 3045–3054, 2001.

[21] Z. Wang, A. C. Bovik, H. R. Sheikh, and E. P. Simoncelli, "Image quality assessment: from error visibility to structural similarity," *IEEE Transactions on Image Processing*, vol. 13, no. 4, pp. 600–612, 2004.